Optica Applicata, Vol. XLI, No. 3, 2011

Optical switch based on cascaded SOI nonlinear directional coupler

QING TAO*, FENGGUANG LUO*, DUSI CAI, QIANLIANG LIANG,
ZHENGWEN WAN, XINMING SONG, XUECHAO LIU

Wuhan National Laboratory for Optoelectronics, School of Optoelectronic Science and Engineering, Huazhong University of Science and Technology, Wuhan 430074, China

*Corresponding authors: Q. Tao – taoqing107@yahoo.com.cn; F. Luo – fgluo@mail.hust.edu.cn.

In this paper, we calculate three effective refractive indexes for cascaded silicon-on-insulator (SOI) nonlinear directional coupler. For each effective refractive index, the coupling length L_C, core-to--distance-ratio K and switching threshold power $P_{i,m}$ are calculated, respectively. However, there are some fabrication errors, which are ΔW, ΔH, ΔK in the height of Si layer and width of Si layer and error of core-to-distance-ratio. We have analyzed the influence of power transmission efficiency $T_{i,j}$ and relative transmission efficiency error $\Delta_{i,j}$ caused by the change of ΔW, ΔH, ΔK. Furthermore, we find the tolerance range of ΔW, ΔH, ΔK for $T_{i,j}$ and $\Delta_{i,j}$ in couplers *a*, *b*, *c*. The other four input pulses with different powers are switched to four different ports. Although output pulses show some little compression and loss, the value of η is very small and output pulse waveforms are not affected seriously. The basic switching function has been realized, so this design is proved to be effective.

Keywords: silicon-on-insulator (SOI), vector finite element, discrete split-step multi-wavelet transformation, coupled nonlinear Schrödinger equation (CNLSE).

1. Introduction

Silicon-on-insulator (SOI) waveguides [1] have attracted great attention lately because they can be used to produce all kinds of optical devices. Owing to the significant third-order nonlinearity and a tight mode confinement, some optical functions can be realized at relatively low input power. Optical pulses have many applications in the SOI waveguides, such as optical switching.

In this paper, we propose a new design of cascaded SOI nonlinear directional coupler, which can be used as a 1×4 optical switch. Three effective refractive indexes are calculated for square SOI waveguide. For each effective refractive index, we adjust the core-to-distance-ratio K_i and coupling length L_{Ci} to fabricate a nonlinear directional coupler. However, there are some fabrication errors, which are ΔW, ΔH, ΔK in the height of Si layer and width of Si layer and error of core-to-distance-ratio. We have analyzed the change of power transmission efficiency $T_{i,j}$ and relative transmission efficiency error $\Delta_{i,j}$ corresponding to different ΔW, ΔH, ΔK. Finally, we obtain

the fabrication tolerance of ΔW, ΔH, ΔK for couplers *a*, *b*, *c*. The other four input pulses with different powers are switched to four different ports. Although output pulses show some little compression and amplitude loss, the amplitude error η is very small and output pulse waveforms do not deform seriously. The basic switching function has been realized, thus this design is effective.

2. Theoretical mode

For symmetrical two-core SOI nonlinear directional couplers, including loss terms and ignoring the effects of gain terms, high order dispersion and saturated gain term, the coupled nonlinear Schrödinger equations (CNLSEs) [2] can be normalized as follows:

$$i\frac{\partial u_1}{\partial \xi} + \frac{1}{2}\frac{\partial^2 u_1}{\partial \tau^2} + |u_1|^2 u_1 + Q_0 u_2 + i\frac{\alpha}{2}u_1 = 0 \tag{1a}$$

$$i\frac{\partial u_2}{\partial \xi} + \frac{1}{2}\frac{\partial^2 u_2}{\partial \tau^2} + |u_2|^2 u_2 + Q_0 u_1 + i\frac{\alpha}{2}u_2 = 0 \tag{1b}$$

where $u_1 = \gamma L_D^{1/2} A_1$ and nonlinear parameter $\gamma = 0.7601$ W/m, the initial amplitude

$$A_1(0, t) = A_0 \exp\left[-\frac{1-2i}{2}\left(\frac{t}{T_0}\right)^2\right] \tag{2}$$

in the first core $t \in [-4096\times10^{-15}$ s, 4096×10^{-15} s]. Input power $P_0 = 0.0745P_1$ W and $A_0 = \sqrt{P_0}$. Power loss $\alpha = 2.30$ dB/km. The initial value $u_2 = 0$ in the second core. $Q_D = \kappa_0 L_D$ is the normalized linear coupling coefficient, $L_D = T_0^2/|\beta_2|$ is the dispersion length with $\beta_2 = -2.15\times10^{-24}$ s^2/m, and $T_0 = 0.125\times10^{-12}$ s is an input pulse width. Here, $\xi = z/L_D$ and $\tau = (t - z/v_g)/T_0$ are the normalized distance and retarded time coordinates, respectively. v_g is the group velocity, wavelength $\lambda = 1.55\times10^{-6}$ m.

The power transmission efficiency $T_{i,j}$ is a function of the pulse energies [3]

$$T_{i,j} = \frac{\int_{-\infty}^{+\infty} |u_{i,j}(L_C, \tau)|^2 \mathrm{d}\tau}{\int_{-\infty}^{+\infty} |u_{1,f}(0, \tau)|^2 \mathrm{d}\tau} \times 100\% \tag{3}$$

$i = 1, 2$; $j = \pm a, \pm b, \pm c, \pm d, \pm e, f$; $a = 0.02$, $b = 0.04$, $c = 0.06$, $d = 0.08$, $e = 0.1$, $f = 0$. Here, *a*, *b*, *c*, *d*, *e* and *f* correspond to different values of ΔK; L_C is the coupling

length. The relative power transmission efficiency error $\Delta_{i,j}$ caused by ΔK is $\Delta_{i,j} = |T_{i,j} - T_{i,f}|/T_{i,f} \times 100\%$. The relative power transmission efficiency error Δ caused by ΔW, ΔH is $\Delta = |T_{i,\Delta W,\Delta H} - T_{i,0,0}|/T_{i,0,0} \times 100\%$; ΔW, ΔH = 0, ±0.01 μm, ±0.02 μm, ±0.03 μm.

3. Numerical method

In general, dispersion and nonlinear effects act jointly along the direction of optical transmission. We derive an approximate result by assuming that dispersion and nonlinear effects act at a short distance, respectively.

Considering only dispersion effects from ξ to $\xi + h/2$ and from $\xi + h/2$ to $\xi + h$, we have

$$\frac{\partial u_1}{\partial \xi} = \frac{i}{2}\frac{\partial^2 u_1}{\partial \tau^2} + iQ_0 u_2 + \Gamma u_1 \tag{4a}$$

$$\frac{\partial u_2}{\partial \xi} = \frac{i}{2}\frac{\partial^2 u_2}{\partial \tau^2} + iQ_0 u_1 + \Gamma u_2 \tag{4b}$$

Considering only the nonlinear effects of the whole length h, we obtain

$$\frac{\partial u_1}{\partial \xi} = \frac{i}{2}|u_1|^2 u_1 \tag{5a}$$

$$\frac{\partial u_2}{\partial \xi} = \frac{i}{2}|u_2|^2 u_2 \tag{5b}$$

We can solve them in three steps; in the fist step, from ξ to $\xi + h/2$, we take the discrete split-step multi-wavelet transformation (DSSMWT) [4, 5] of Eqs. (4),

$$\mathrm{MW}\tilde{u}_{1,\xi+h/2} = \mathrm{MW}\exp\left(\frac{h\hat{L}}{2}\right)u_{1,\xi}$$

$$\mathrm{MW}\tilde{u}_{2,\xi+h/2} = \mathrm{MW}\exp\left(\frac{h\hat{L}}{2}\right)u_{2,\xi}$$

where $\tilde{u}_1$ and $\tilde{u}_2$ are the DSSMWT of u_1 and u_2, respectively. MW represents the multi-wavelet transform operation.

In the second step, taking the nonlinear effects of the whole length h, the nonlinear part is solved in the time domain by the following method

$$u_{1\mathrm{NL}}\left(\xi+\frac{h}{2},\,\tau\right) = \mathrm{IDSSMWT}\left[\tilde{u}_{1,\,\xi+\frac{h}{2}}\right]\exp\left[\frac{ih\left(\left|u_1(\xi,\,\tau)\right|^2+\left|u_1(\xi+h,\,\tau)\right|^2\right)}{2}\right] \tag{6a}$$

$$u_{2\mathrm{NL}}\left(\xi+\frac{h}{2},\,\tau\right) = \mathrm{IDSSMWT}\left[\tilde{u}_{2,\,\xi+\frac{h}{2}}\right]\exp\left[\frac{ih\left(\left|u_2(\xi,\,\tau)\right|^2+\left|u_2(\xi+h,\,\tau)\right|^2\right)}{2}\right] \tag{6b}$$

IDSSMWT denotes the inverse discrete split-step multi-wavelet transformation.

In the third step, considering only the action from $\xi + h/2$ to $\xi + h$ and making similar DSSMWT calculation to solve Eqs. (4), we have

$$\mathrm{MW}\tilde{u}_{1\mathrm{NL},\,\xi+h} = \mathrm{MW}\exp\left(\frac{h\hat{L}}{2}\right)u_{1\mathrm{NL},\,\xi+h/2}$$

$$\mathrm{MW}\tilde{u}_{2\mathrm{NL},\,\xi+h} = \mathrm{MW}\exp\left(\frac{h\hat{L}}{2}\right)u_{2\mathrm{NL},\,\xi+h/2}$$

Finally, at the output position of $\xi + h$, we obtain

$$u_1(\xi+h,\,\tau) = \mathrm{IDSSMWT}\left[\tilde{u}_{1\mathrm{NL},\,\xi+h}\right] \tag{7a}$$

$$u_2(\xi+h,\,\tau) = \mathrm{IDSSMWT}\left[\tilde{u}_{2\mathrm{NL},\,\xi+h}\right] \tag{7b}$$

4. Design of SOI directional coupler

A cascaded SOI nonlinear directional coupler can be designed to form an optical switch, as shown in Fig. 1. Because the cross-section of the core and cladding layer are square, respectively, the side length of Si layer is $W = H = 0.6$ μm, the side length of SiO_2 layer is $W_1 = H_1 = 1.2$ μm. The relative refractive index of Si layer is 3.455, and the relative refractive index of SiO_2 layer is 1.46.

Through vector finite element method [6–8], we can easily get the effective refractive index $n_{\mathrm{eff}} = \beta/k_0$.

Moreover, σ is the core radius, ρ is the distance of two cores, $K = \rho/\sigma$ [9–11]. For coupler *a*, $n_{\mathrm{eff}1} = 2.508288$, $K_1 = 4.5$ and $L_{C1} = 0.0037$ m. For coupler *c*, $n_{\mathrm{eff}3} =$ $= 2.000879$, $K_3 = 4$ and $L_{C3} = 0.0016$ m.

For coupler *b*, $n_{\mathrm{eff}2} = 3.022567$, $K_2 = 5.2$ and $L_{C2} = 0.0075$ m. However, during the production of the coupler, there are some errors in the height of Si layer and width

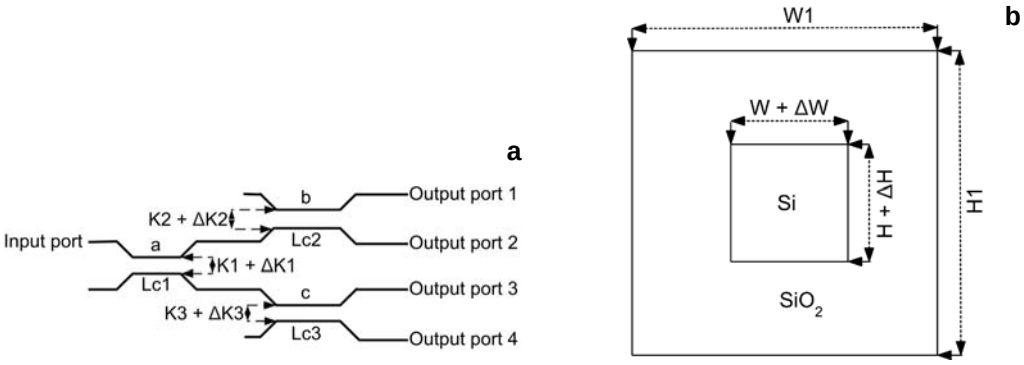

Fig. 1. Cascaded SOI nonlinear optical switch. Optical switch structure diagram (**a**). Cross-section of optical switch (**b**).

of Si layer. ΔW, $\Delta H \in$ [–0.03 μm, 0.03 μm] corresponds to the width error and height error of Si layer. ΔK corresponds to the error of core-to-distance-ratio. $\Delta K_1, \Delta K_2, \Delta K_3 \in$ [–0.1, 0.1], corresponds to the error of core-to-distance-ratio for couplers *a*, *b*, *c*, respectively. The impacts on the power transmission efficiency were analyzed by the change of ΔK and ΔW, and ΔH, as shown in Figs. 2 and 3.

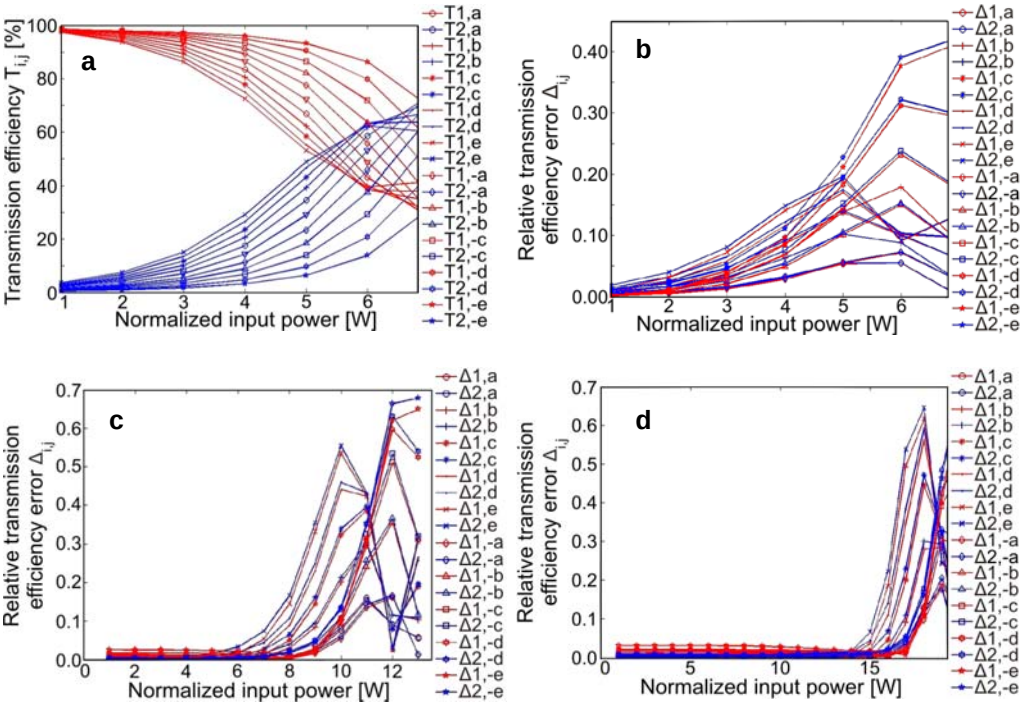

Fig. 2. Transmission efficiency diagrams. Power transmission efficiency corresponding to coupler *c* (**a**). Relative transmission efficiency error corresponding to coupler *c* (**b**). Relative transmission efficiency error corresponding to coupler *a* (**c**). Relative transmission efficiency error corresponding to coupler *b* (**d**).

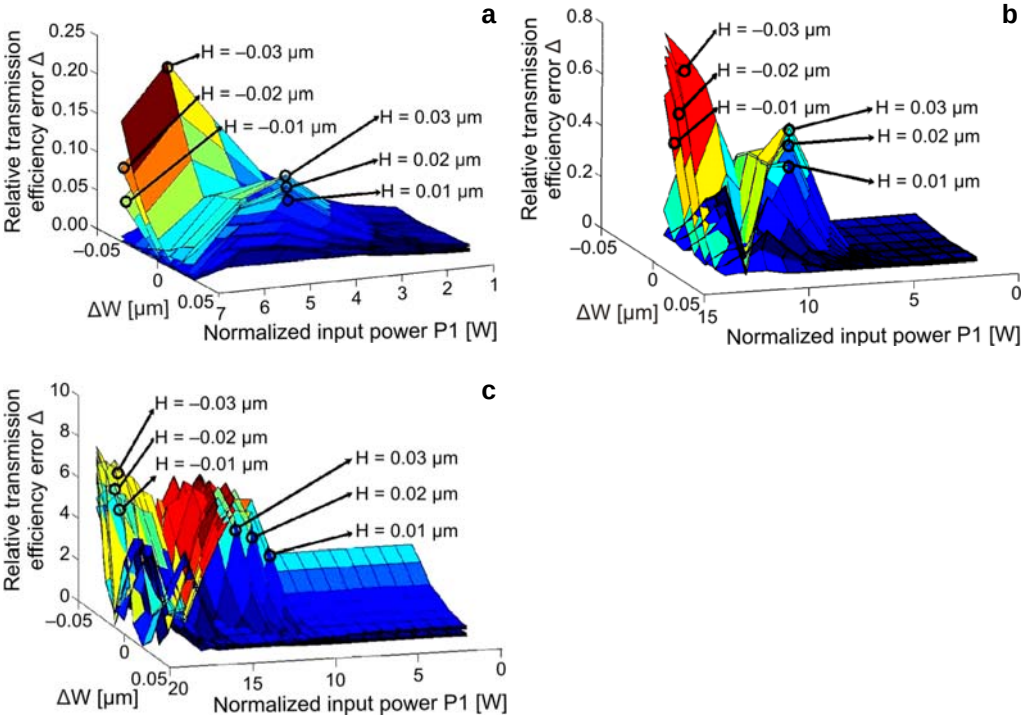

Fig. 3. Transmission efficiency diagrams. Relative transmission efficiency error corresponding to coupler *c* (**a**). Relative transmission efficiency error corresponding to coupler *a* (**b**). Relative transmission efficiency error corresponding to coupler *b* (**c**).

The actual normalized input power threshold value $P_{i,m}$ (i = 1, 2, 3) is easily obtained. For coupler *a*, $P_{1,m}$ = 12 W; for coupler *b*, $P_{2,m}$ = 20 W; moreover, $P_{3,m}$ = 6 W for coupler *c*. One can easily find the changes of $T_{i,j}$ and $\Delta_{i,j}$, when ΔK_3 varies for coupler *c*, as in Figs. 2**a** and 2**b**. When $\Delta K_3 \in$ [–0.04, 0.06], $\Delta_{i,j} < 0.15\%$. There are few impacts on the power transmission. Similarly, Fig. 2**c** reflects the changes of $\Delta_{i,j}$ with ΔK_1 for coupler *a*. Also, there are few impacts on the power transmission. When $\Delta K_1 \in$ [–0.02, 0.04], $\Delta_{i,j} < 0.3\%$. Figure 2**d** describes the changes of $\Delta_{i,j}$ with ΔK_2 for coupler *b*. When $\Delta K_2 \in$ [–0.02, 0.04], $\Delta_{i,j} < 0.3\%$. Still, there are few impacts on the power transmission.

The changes of Δ can be obtained, when ΔW and ΔH vary for couplers *a*, *b*, *c*, as shown in Fig. 3. We can easily find that when $\Delta H < 0$, Δ caused by $\Delta W \in$ [0 μm, 0.03 μm] is less than that caused by $\Delta W \in$ [–0.03 μm, 0 μm]; when $\Delta H > 0$, Δ caused by $\Delta W \in$ [0 μm, 0.03 μm] is more than that by $\Delta W \in$ [–0.03 μm, 0 μm]. When ΔW does not change, Δ increases with the absolute value of ΔH increasing.

For coupler *c*, when $\Delta W \in$ [–0.03 μm, 0.03 μm] and $\Delta H \in$ [–0.02 μm, 0.03 μm], Δ is less than 0.15%. There are few impacts on the power transmission. For coupler *a*, while $\Delta W \in$ [–0.01 μm, 0.02 μm] and $\Delta H \in$ [–0.01 μm, 0.02 μm], Δ is less than 0.4%.

Also, there are few impacts on the power transmission. Furthermore, for coupler *b*, when $\Delta W \in$ [–0.01 μm, 0.02 μm] and $\Delta H \in$ [–0.01 μm, 0.02 μm], Δ is less than 0.4%. Still, there are few impacts on the power transmission.

Finally, when ΔW and ΔH are fixed, $\Delta K_3 \in$ [–0.04, 0.06], $\Delta_{i,j} < 0.15\%$ for coupler *c*; $\Delta K_1 \in$ [–0.02, 0.04], $\Delta_{i,j} < 0.3\%$ for coupler *a*; $\Delta K_2 \in$ [–0.02, 0.04], $\Delta_{i,j} < 0.3\%$ for coupler *b*. Then, during the tolerance of ΔK_i, there are few impacts on the power transmission. When ΔK is fixed, $\Delta W \in$ [–0.03 μm, 0.03 μm] and $\Delta H \in$ [–0.02 μm, 0.03 μm], $\Delta < 0.15\%$ for coupler *c*; $\Delta W \in$ [–0.01 μm, 0.02 μm] and $\Delta H \in$ [–0.01 μm, 0.02 μm], $\Delta < 0.4\%$, for coupler *a*; $\Delta W \in$ [–0.01 μm, 0.02 μm] and $\Delta H \in$ [–0.01 μm, 0.02 μm], $\Delta < 0.4\%$ for coupler *b*. In this way, during the tolerance of ΔW_i and ΔH_i, there are few impacts on the power transmission.

5. Results

Theoretically, when normalized input pulse power $P_1 < P_{3,m}$, the output pulse exports from port 4. When $P_1 > P_{2,m}$, the output pulse exports from port 2. When $P_{3,m} < P_1 < P_{2,m}$, the output pulse exports from port 3. Finally, for $P_{1,m} < P_1 < P_{2,m}$, the output pulse exports from port 1. For the input pulses with different power P_1 = 4, 9, 15, 24 W, we can find respective output pulses in port 4/port 2/port 3/port 1, as shown in Figs. 4–7. We can define the amplitude error η, as follows

$$\eta = \frac{|A_O - A_I|}{A_I} \times 100\%$$

where A_O is the amplitude of output pulse and A_I is the amplitude of input pulse. Because P_1 = 4 W is low compared to the entire normalized input threshold power value, the pulse goes through twice cross coupling and arrives at the port 4. The output pulse has a little compression and the pulse amplitude is reduced, as shown in Fig. 4. But we can easily find that maximum of η is lower than 0.004%, the action of the coupler has little effect on the output pulse.

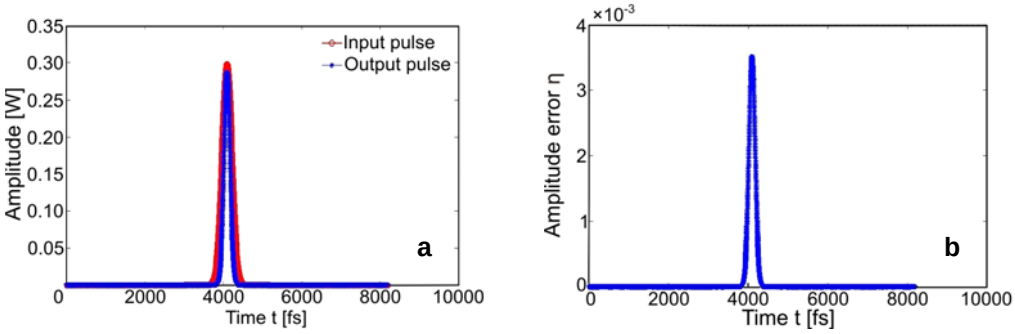

Fig. 4. Input and output pulse (P_1 = 4 W) – **a**. Amplitude error of output pulse in port 4 – **b**.

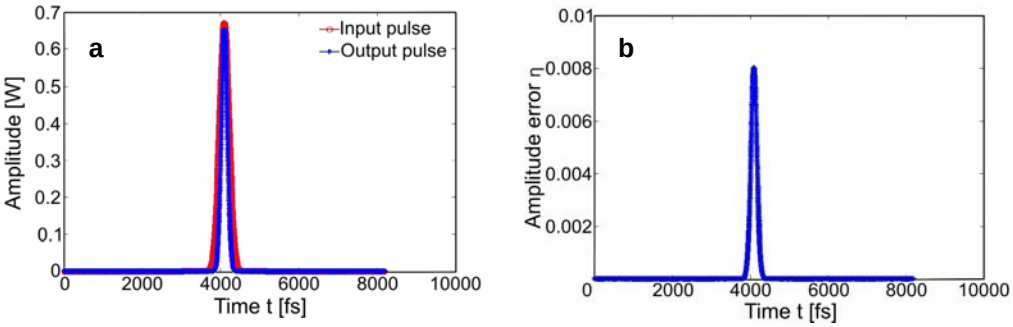

Fig. 5. Input and output pulse (P_1 = 9 W) – **a**. Amplitude error of output pulse in port 3 – **b**.

Similarly, for $P_{3,\,m} < P_1 = 9\ \text{W} < P_{1,\,m}$, the output pulse runs through a cross state in the coupler *a* and bar state in the coupler *c*. The output pulse still has a little compression and the pulse amplitude is reduced and arrives at the port 3, as shown in Fig. 5.

However, one can easily see that the maximum of η is lower than 0.008%, the function of the coupler has hardly any effect on the output pulse.

When $P_{1,\,m} < P_1 = 15\ \text{W} < P_{2,\,m}$, the output pulse goes through a bar state in the coupler *a* and cross state in the coupler *c*. Then, it arrives at the port 1. The output

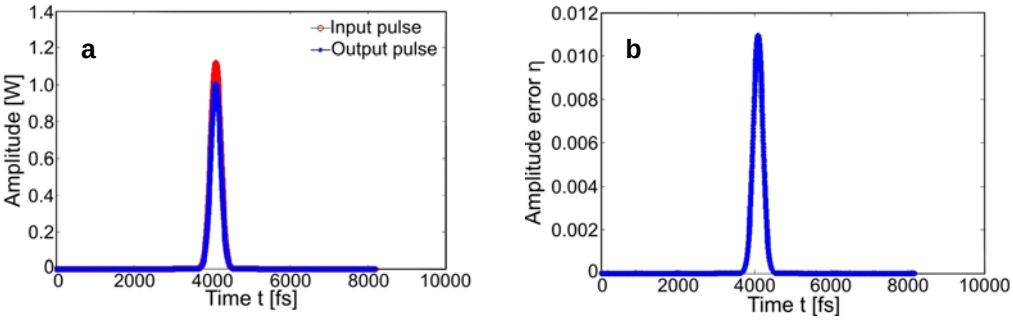

Fig. 6. Input and output pulse (P_1 = 15 W) – **a**. Amplitude error of output pulse in port 1 – **b**.

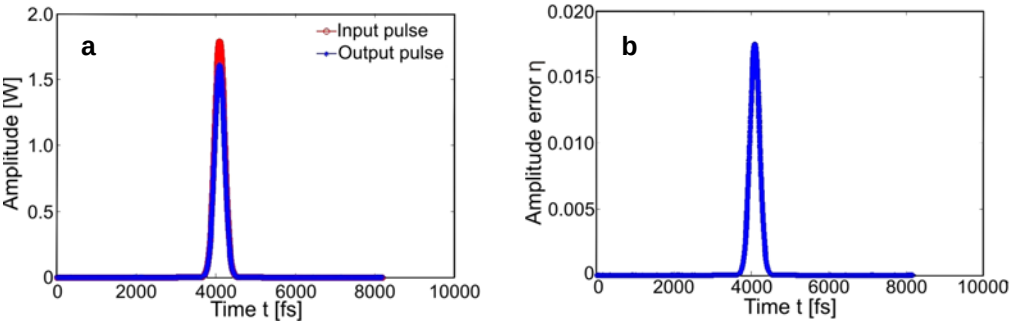

Fig. 7. Input and output pulse (P_1 = 24 W) – **a**. Amplitude error of output pulse in port 2 – **b**.

pulse also has a little compression and the pulse amplitude is reduced, as described in Fig. 6. But, one can easily see that the maximum of η is lower than 0.012%, the action of the coupler has little effect on the output pulse.

Similarly, when $P_{2,m} < P_1 = 24$ W, the output pulse runs through twice bar coupling. Afterwards, it arrives at the port 2. The output pulse still has a little compression and pulse amplitude is reduced, as depicted in Fig. 7. However, it can be easily seen that the maximum of η is lower than 0.018%, the function of the coupler has also little effect on the output pulse.

Finally, although the output pulses have some little compression and amplitudes of pulses are reduced, the value of η is very small and the output pulse waveforms are not affected seriously. The basic switching function has been realized, so this design is proved to be effective.

6. Conclusions

In this paper, we have calculated three effective refractive indexes for cascaded SOI coupler. For each effective refractive index, the coupling length L_C, core-to-distance--ratio K and switching threshold power $P_{i,m}$ are calculated, respectively. However, when really fabricating these couplers, there are some errors, which are ΔW, ΔH, ΔK in the height of Si layer and the width of Si layer and the error of core-to-distance--ratio. We have analyzed the change of power transmission efficiency $T_{i,j}$ and relative transmission efficiency error $\Delta_{i,j}$ caused by the change of ΔW, ΔH, ΔK. Furthermore, we have found the tolerance range of ΔW, ΔH, ΔK for the $T_{i,j}$ and $\Delta_{i,j}$ in the couplers *a*, *b*, *c*. The four input pulses with different power are switched to four different ports. Although the output pulses have some little compression and loss, the value of η is very small and the output pulse waveforms are not affected seriously. The basic switching function has been realized, so this design is effective.

References

[1] SARMA A.K., *Silicon waveguide based nonlinear directional coupler as a soliton switch*, Optical Engineering **47**(12), 2008, p. 120503.

[2] QILIANG LI, YUYONG XIE, YINFANG ZHU, YONGMIN QI, ZHIJING ZHAO, *Effects of second-order coupling coefficient dispersion on short-pulse propagation and switching in an active two-core nonlinear fiber coupler*, Journal of Lightwave Technology **27**(15), 2009, pp. 2933–2940.

[3] DA SILVA M.G., BASTOS A.M., SOBRINHO C.S., LIMA J.L.S., DE ALMEIDA E.F., SOMBRA A.S.B., *Optical crosstalk in a periodically inhomogeneous nonlinear dispersion directional fiber coupler*, Optical Fiber Technology **11**(2), 2005, pp. 180–192.

[4] PIERCE I., SHORE K.A., *Modelling pulse propagation in semiconductor optical amplifiers using wavelets*, IEE Proceedings Optoelectronics **145**(1), 1998, pp. 88–92.

[5] SUMESH E.P., ELIAS E., *Multiwavelet optimized finite difference method to solve nonlinear Schrödinger equation in optical fiber*, TENCON 2008 – IEEE Region 10 Conference, November 19–21, 2008, pp. 1–6.

[6] FISHER A., WHITE D., RODRIGUE G., *An efficient vector finite element method for nonlinear electromagnetic modeling*, Journal of Computational Physics **225**(2), 2007, pp. 1331–1346.

[7] VOLLAIRE C., MUSY F., PERRUSSEL R., *Post processing for the vector finite element method: Accurate computing of dual field*, IEEE Transactions on Magnetics **42**(4), 2006, pp. 819–822.
[8] AL SALAMEH M.S., AL ZURAIQI E.T., *Solutions to electromagnetic compatibility problems using artificial neural networks representation of vector finite element method*, IET Microwaves, Antennas and Propagation **2**(4), 2008, pp. 348–357.
[9] KIN S. CHIANG, *Intermodal dispersion in two-core optical fibers*, Optics Letters **20**(9), 1995, pp. 997–999.
[10] YOUFA WANG, WENFENG WANG, *Nonlinear optical pulse coupling dynamics*, Journal of Lightwave Technology **24**(6), 2006, pp. 2458–2464.
[11] DROULIAS S., MANOUSAKIS M., HIZANIDIS K., *Switching dynamics in nonlinear directional fiber couplers with intermodal dispersion*, Optics Communications **240**(1–3), 2004, pp. 209–219.

Received July 13, 2010
in revised form September 27, 2010